
Text-to-Image Rectified Flow as Plug-and-Play Priors

Xiaofeng Yang

College of Computing and Data Science
Nanyang Technological University
Singapore
yang.xiaofeng@ntu.edu.sg

Cheng Chen

College of Computing and Data Science
Nanyang Technological University
Singapore

Xulei Yang

Institute for Infocomm Research
A*STAR
Singapore

Fayao Liu

Institute for Infocomm Research
A*STAR
Singapore

Guosheng Lin*

College of Computing and Data Science
Nanyang Technological University
Singapore
gslin@ntu.edu.sg

Abstract

Large-scale diffusion models have achieved remarkable performance in generative tasks. Beyond their initial training applications, these models have proven their ability to function as versatile plug-and-play priors. For instance, 2D diffusion models can serve as loss functions to optimize 3D implicit models. Rectified flow, a novel class of generative models, enforces a linear progression from the source to the target distribution and has demonstrated superior performance across various domains. Compared to diffusion-based methods, rectified flow approaches surpass in terms of generation quality and efficiency, requiring fewer inference steps. In this work, we present theoretical and experimental evidence demonstrating that rectified flow based methods offer similar functionalities to diffusion models — they can also serve as effective priors. Besides the generative capabilities of diffusion priors, motivated by the unique time-symmetry properties of rectified flow models, a variant of our method can additionally perform image inversion. Experimentally, our rectified flow-based priors outperform their diffusion counterparts — the SDS and VSD losses — in text-to-3D generation. Our method also displays competitive performance in image inversion and editing. Code is available at: https://github.com/yangxiaofeng/rectified_flow_prior.

1 Introduction

Large-scale diffusion models [1; 2; 3; 4] have made significant advances in recent years. Applications in image generation [4; 5; 6; 7; 8], video creation [9; 10], and music production [11] have shown superior performance compared to traditional Generative Adversarial Networks (GANs) [12]. In addition to excelling in tasks for which they are specifically trained, various studies [13; 14; 15; 16] indicate that these models can also serve as plug-and-play priors for related tasks, i.e., using the pretrained diffusion models as loss functions. For example, Dreamfusion [14] introduces the SDS

*Corresponding Author

loss, utilizing a pretrained text-to-image diffusion model to generate 3D objects. DDS [17] extends the original SDS loss to address image editing challenges. Various subsequent works [15; 16; 18; 19] further refine the SDS loss to enhance generation quality and diversity.

Rectified flow [20; 21; 22] is a new type of flow-based generative model that linearly transfers the source distribution to the target distribution. This property of linear transfer facilitates simulation-free training and faster sampling at inference time. Recently, methods based on rectified flow have garnered considerable research interest. Initial work such as InstalFlow [23] has been capable of generating high-quality images in just a few inference steps. More recent developments, like rectified flow based stable diffusion [24], have achieved new state-of-the-art performance in image generation. Given the growing research focus, it remains to be seen whether large-scale pretrained rectified flow models can function as effective priors, similar to diffusion-based methods.

In this work, we explore how to distill knowledge from pretrained text-to-image rectified flows and use them as priors for other tasks. We propose three methods. The first, named RFDS (**R**ectified **F**low **D**istillation **S**ampling), is intended to serve as a baseline method for rectified flow priors, analogous to the SDS loss in diffusion models. Specifically, we derive the baseline RFDS by calculating the gradients of the input image by reversing the rectified flow training process. We observe a similar phenomenon to that seen in diffusion-based methods: by removing the Jacobian of the rectified flow U-Net, RFDS can generate meaningful images or 3D objects given text conditions.

Moreover, an intriguing characteristic of rectified flow is its linear trajectory between the initial Gaussian distribution and the image distribution, a property known as the time-symmetry property. Inspired by this characteristic, we notice that the baseline RFDS can be easily extended to optimize randomly sampled noise by taking the negative gradient of the original RFDS. We refer to this method as iRFDS, which represents the inverse of RFDS. Optimizing noise is crucial for tasks like image inversion and editing. Typically, an image editing problem involves identifying the original noise of a given real image and subsequently altering the text prompt to edit the image. Our experiments demonstrate that iRFDS is effective at performing image inversion and editing on real-world images.

Finally, we introduce RFDS-Rev (RFDS Reversal) to enhance the generation quality of the baseline RFDS loss. Our observations reveal that the original RFDS loss exhibits behaviors similar to those of the SDS loss, such as limited detail and diversity in generated content. We attribute these issues to the mode-seeking tendency of the RFDS loss due to random sampling. As rectified flow learns a unique mapping for each noise input, the RFDS leads to averaged images with diminished detail when random noise sampling is used. To address these challenges, we propose RFDS-Rev, which iteratively applies the iRFDS for flow reversal to determine the original noise, and RFDS for knowledge distillation to refine the input. Experimentally, we find that the RFDS-Rev method significantly outperforms both the RFDS baseline and the diffusion-based VSD loss.

Our experiments are carried out on 2D image inversion and editing for iRFDS and text-to-3D generation for RFDS and RFDS-Rev. Notably, the RFDS-Rev method achieves a new state-of-the-art performance in text-to-3D benchmarks among all 2D lifting methods, surpassing a broad spectrum of diffusion priors. Some generation results can be found in Fig. 1.

To summarize our contributions:

- We propose the first series of studies that utilize pretrained rectified flow models as priors. Our methods span a wide array of applications, from generative tasks such as text-to-3D generation to the inversion and editing of real images.
- Compared to diffusion-based priors, our methods significantly outperform them in text-to-3D generation and achieve highly competitive results in image inversion and editing.

2 Preliminaries: Rectified Flow

The idea of rectified flow is proposed in multiple concurrent works [20; 21; 22]. Here, we follow the interpretation of [20] to briefly introduce the basic concepts of rectified flow.

Rectified flow is an ordinary differentiable equation model that defines the transportation from π_0 to π_1 to follow a straight line. Its general form is defined as:

$$dZ_t = v(Z_t, t)dt. \quad (1)$$

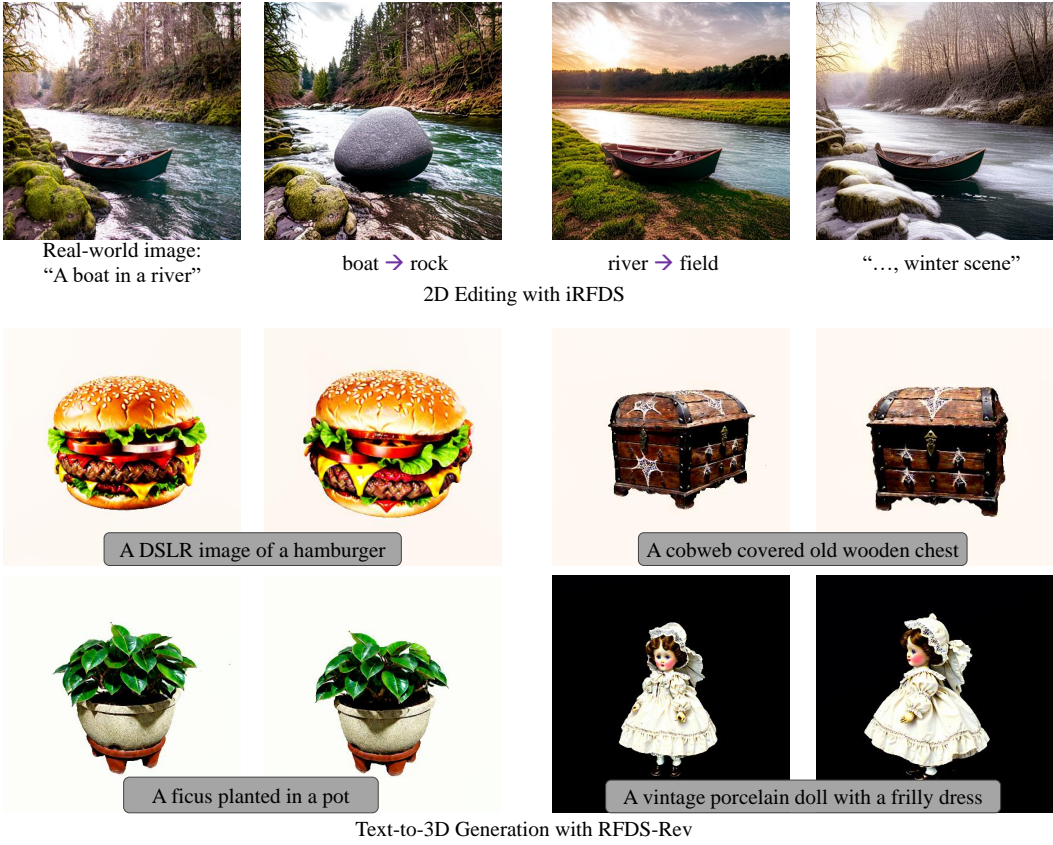


Figure 1: Demonstration of potential use cases of the proposed rectified flow priors. Our methods can be used on 2D inversion and editing and text-to-3D generation.

Given two data points sampled from the two distributions: $X_0 \sim \pi_0$, $X_1 \sim \pi_1$. The drift force v is set to learn the difference between the two data points:

$$\min_{\phi} \int_0^1 \mathbb{E} [\| (X_1 - X_0) - v_{\phi}(X_t, t) \|^2] dt, \text{ with } X_t = tX_1 + (1 - t)X_0. \quad (2)$$

Practically, the drift force v is parameterized using neural networks with parameters ϕ . Once the network is trained with the above loss function, data points in the target distribution can be recovered by following the ODE process in just a few steps along straight flow lines.

However, it is important to note that the primary objective of this work is not to recover the original data points (e.g., generating images using rectified flow networks). Instead, our aim is to distill knowledge from such pretrained networks—specifically by employing the pretrained network as a loss function—to enhance the functionality of text-to-image networks across a wider array of applications, including image editing and text-to-3D generation.

Our proposed method is also related to diffusion-based priors. We discuss these related works in the Appendix.

3 Methods

In this section, we discuss the three proposed distillation methods: the RFDS (Rectified Flow Distillation Sampling) baseline method, the iRFDS (inverse RFDS) method for image inversion and finally the RFDS-Rev (RFDS-Reversal) method to improve the generation quality of baseline RFDS.

Formulation. The problem of optimization using pretrained rectified flow models as loss functions can be formatted as follows: we would like to optimize $x = g(\theta)$ given $\theta^* = \operatorname{argmin}_{\theta} \mathcal{L}_{\text{RF}}(\phi, x = g(\theta))$. The form of x can be Neural Radiance Field or 3D Gaussian Splitting in 3D generation

problem, where the parameter θ denotes the parameters of the 3D models. In the 2D case, x is directly θ . In the remaining of this section, we prove how to define the \mathcal{L}_{RF} and find its gradients related to θ .

3.1 RFDS

Consider the training loss function of rectified flow in Eq. 2. Using the pretrained rectified flow network as a loss function can be seen as an inverse operation of the training process; that is, optimizing the input rather than the model parameters. Specifically, when we place the optimization variable x in the aforementioned equation, it transforms as follows:

$$\min_{\theta} \int_0^1 \mathbb{E} [\| x - \epsilon - v_{\phi}(x_t, t) \|^2] dt, \text{ with } x = g(\theta) \text{ and } x_t = tx + (1-t)\epsilon. \quad (3)$$

Here, the rectified flow network parameter ϕ is fixed and ϵ is a randomly sampled noise.

To find θ , the gradients of the above equation with respect to θ can be written as:

$$\nabla_{\theta} \mathcal{L}_{\text{RF}}(\phi, x, \epsilon, t) = 2 \times \mathbb{E} \left[\underbrace{(x - \epsilon - v_{\phi}(x_t, t))}_{\text{Rf Residual}} \frac{\partial(x - \epsilon - v_{\phi}(x_t, t))}{\partial x} \underbrace{\frac{\partial x}{\partial \theta}}_{\text{Generator Jacobian}} \right]. \quad (4)$$

It could be further simplified as:

$$\nabla_{\theta} \mathcal{L}_{\text{RF}}(\phi, x, \epsilon, t) = 2 \times \mathbb{E} \left[\underbrace{(x - \epsilon - v_{\phi}(x_t, t))}_{\text{Rf Residual}} \left(\underbrace{\frac{\partial(x - \epsilon)}{\partial x}}_{\text{Positive Constant}} - \underbrace{\frac{\partial v_{\phi}(x_t, t)}{\partial x_t} \frac{\partial x_t}{\partial x}}_{\text{Rf network Jacobian}} \right) \underbrace{\frac{\partial x}{\partial \theta}}_{\text{Generator Jacobian}} \right]. \quad (5)$$

As highlighted in diffusion-based methods [14], calculating the network Jacobian is computationally expensive and reacts inadequately to low levels of noise. We observe similar behaviors in models based on rectified flow. Consequently, we also choose to disregard the rectified flow network Jacobian by setting it to identity matrix, akin to the approach taken with diffusion priors. This modification leads to the final RFDS loss:

$$\nabla_{\theta} \mathcal{L}_{\text{RF}}(\phi, x, \epsilon, t) \simeq \mathbb{E} \left[w(t) \underbrace{(x - \epsilon - v_{\phi}(x_t, t))}_{\text{Rf Residual}} \underbrace{\frac{\partial x}{\partial \theta}}_{\text{Generator Jacobian}} \right]. \quad (6)$$

Here we use $w(t)$ to represent a positive value related to timestep $t \in [0, 1]$, and it absorbs all constant values in Eq. 5. The RFDS loss is able to use the pretrained rectified flow model as a loss function to optimize any given image x . Detailed algorithm of RFDS is included in the Appendix.

3.2 iRFDS

A particularly useful and intriguing characteristic of rectified flow models is their time-symmetry property [20]. This allows the models to flow from noise to image and also from image back to noise. Motivated by this property, we observe that if our optimization objective changes from the input image $x = g(\theta)$ to the noise ϵ , Eq. 5 now becomes:

$$\nabla_{\epsilon} \mathcal{L}_{\text{RF}}(\phi, x, \epsilon, t) = 2 \times \mathbb{E} \left[\underbrace{(x - \epsilon - v_{\phi}(x_t, t))}_{\text{Rf Residual}} \left(\underbrace{\frac{\partial(x - \epsilon)}{\partial \epsilon}}_{\text{Negative Constant}} - \underbrace{\frac{\partial v_{\phi}(x_t, t)}{\partial x_t} \frac{\partial x_t}{\partial \epsilon}}_{\text{Rf network Jacobian}} \right) \right]. \quad (7)$$

Since the gradient is now calculated with respect to ϵ , the term of $\frac{\partial(x - \epsilon)}{\partial \epsilon}$ will become negative. Therefore, the final form of iRFDS can be represented as:

$$\nabla_{\epsilon} \mathcal{L}_{\text{RF}}(\phi, x, \epsilon, t) \simeq \mathbb{E} \left[-w(t) \underbrace{(x - \epsilon - v_{\phi}(x_t, t))}_{\text{Rf Residual}} \right]. \quad (8)$$

Optimizing and recovering the original noise from an image is crucial for image inversion and editing problems. By first retrieving the original noise and subsequently modifying the caption, we demonstrate in the experiment section that our method can effectively edit real-world images. Detailed algorithm of iRFDS is included in the Appendix.

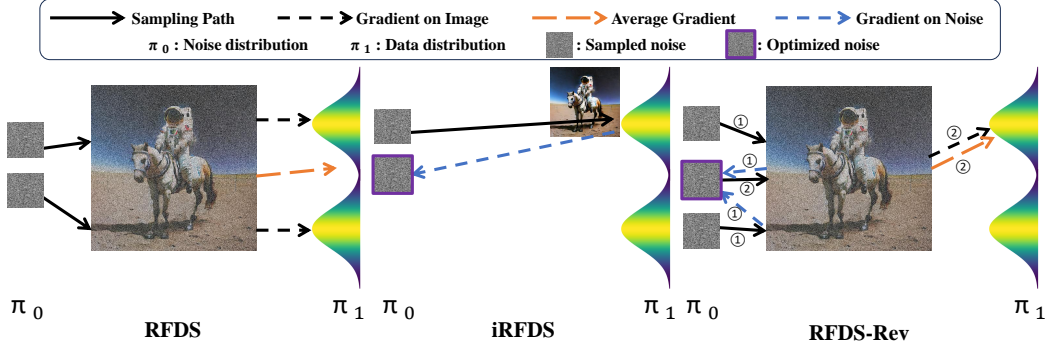


Figure 2: Illustration of our proposed methods.

3.3 RFDS-Rev

RFDS-Reversal (RFDS-Rev) is designed to enhance the baseline RFDS in terms of generation quality. We observe that the RFDS method encounters issues similar to those found with the SDS loss, such as a lack of object details. While several approaches, like the VSD loss, have been proposed to improve the SDS loss and some are applicable to rectified flows, none shows effective results with rectified flow models based on our experiments.

To enhance the baseline RFDS, we draw inspiration from the learning mechanisms of rectified flows. It is important to recall that rectified flow essentially learns an optimal transport from the original noise distribution to the image distribution using straight flows [20]. The mode-seeking nature of the original RFDS, which scans different noises, leads to an averaged velocity and consequently blurred images. As shown on the left side of Fig. 2, when two noise points are sampled, although both give gradients towards the high-density areas in the image domain, the averaged gradient does not necessarily point in the correct direction. To address this issue, we first introduce a critical assumption:

Assumption 1: Given a sample X_1 from data distribution π_1 , there is at most one corresponding X_0 from noise distribution π_0 that is coupled with X_1 .

This assumption is straightforward, as the training process for rectified flow enforces a linear, non-crossing flow [20]. Based on this assumption, we propose RFDS-Reversal (RFDS-Rev), a two-stage method to improve the baseline RFDS. Specifically, as depicted on the right in Fig. 2, the first stage performs noise reversal. In the first stage, we use iRFDS to optimize each randomly sampled noise such that their reversal occupies a relatively static position within the noise distribution. Once the reversal is determined, in the second stage, we apply RFDS to the reversed noise. The algorithm of RFDS-Rev is summarized in Algorithm 1. In experiments, we observe that running iRFDS for just one step yields very satisfactory results. Unless specified otherwise, the experiments involving RFDS-Rev employ $n = 1$ as the default configuration.

Algorithm 1: The RFDS-Rev Algorithm.

```

1 Initialize the learnable parameter  $\theta$ 
2 while Not Converge do
3   Sample random timestep  $t$ 
4   Sample random noise  $\epsilon$ 
5   for  $n$  steps do
6     | Freeze  $\theta$ , optimize  $\epsilon$  with iRFDS (Eq. 8)
7   | Optimize  $\theta$  with optimized  $\epsilon$  based on RFDS (Eq. 6)
8 RETURN  $\theta$ 

```



Figure 3: 2D Comparison. Text Prompts: A castle next to a mountain. An astronaut is riding a horse. A monster truck.

3.4 Classifier Free Guidance

The above equations are derived using the rectified flow network v_ϕ . In practice, since the base rectified flow model [23] is trained with classifier free guidance [25], we observe that using a classifier free guidance version of the network \hat{v}_ϕ help to improve the performance. Ablation experiments of this problem are included in the Appendix.

4 Experiments

In this section, we conduct extensive experiments to compare our proposed methods with diffusion-based methods. Firstly, we focus on evaluating RFDS and RFDS-Rev in both 2D and 3D text-guided generation scenarios. Subsequently, we explore the performance of iRFDS in image inversion tasks. Unless otherwise noted, our rectified flow experiments utilize the large-scale text-to-image model InstaFlow [23]. For comparison, the diffusion-based methods are implemented using Stable Diffusion v2.1 [4] and Threestudio codebase [26]. In terms of base model generation FID, the rectified flow based model InstaFlow [23] that we used is slightly weaker compared to Stable Diffusion. We include the implementation details in the Appendix for further reference.

4.1 RFDS vs. RFDS-Rev vs. Diffusion Priors

Toy Experiments on Optimization of 2D Case. We first conduct an intuitive experiment in the 2D setting by setting $x = \theta$. This setup removes the complexity of the 3D model, thereby showcasing the potential upper limit of 3D generation quality. We compare two of our proposed methods, the RFDS baseline and RFDS-Rev, against diffusion-based methods. Results are depicted in Fig. 3. We observe that our proposed baseline method, RFDS, achieves performance comparable to that of the diffusion-based SDS loss. With just one additional forward pass, our RFDS-Rev method significantly enhances the generation quality over the baseline RFDS. RFDS-Rev manages to produce very competitive results compared to VSD.

Text-to-3D Generation by Lifting 2D Models. An important application of rectified flow or diffusion priors is lifting models from 2D to 3D. We present both quantitative and qualitative results for text-to-3D generation. The qualitative results are displayed in Fig. 4. We observe that both of our proposed methods are capable of generating high-quality 3D objects, with the RFDS-Rev method enhancing the baseline RFDS in terms of object detail and color accuracy. Qualitatively, the RFDS baseline shows competitive performance than the SDS loss used in diffusion-based methods. Compared to VSD, RFDS-Rev achieves a comparable level of detail in generated objects. Notably, VSD experiences issues with “exploding” artifacts, as highlighted in the red box in our figures. In contrast, the RFDS-Rev loss does not exhibit this problem. Additional qualitative results of RFDS-Rev are included in the Appendix.

We also conduct quantitative experiments on text-to-3D benchmark T³Bench [27]. Results are demonstrated in Table 1. We observe that our proposed methods significantly outperform diffusion-

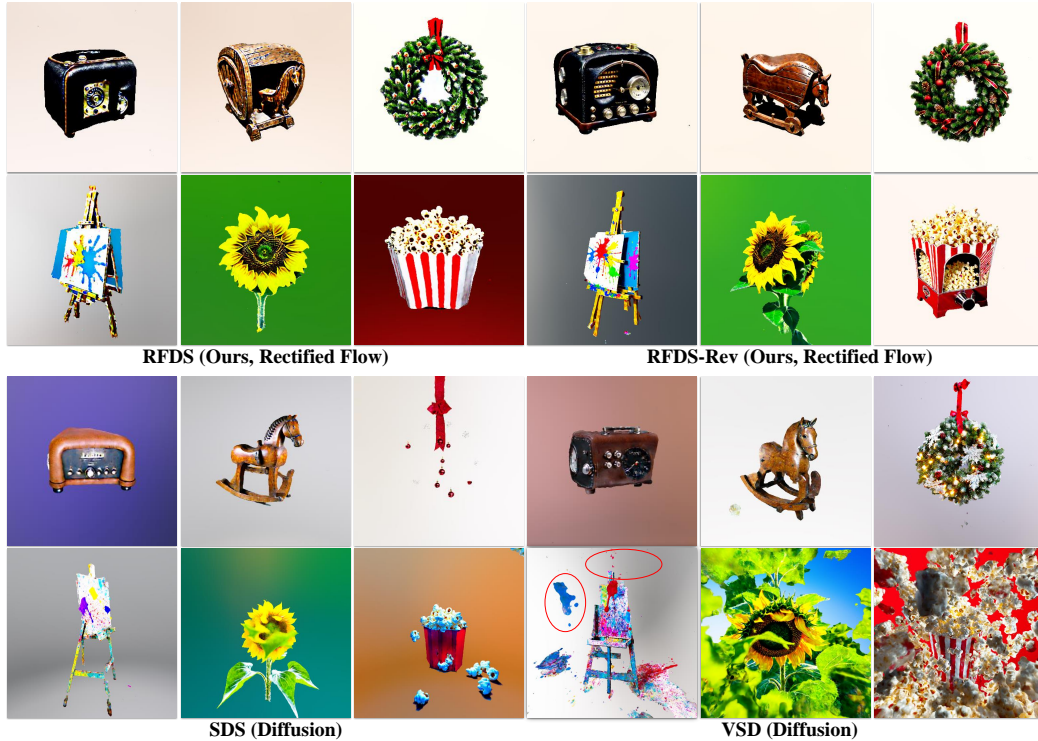


Figure 4: 3D Comparison. Text Prompts: A classic leatherette radio with dials, An antique wooden rocking horse, A fragrant pine Christmas wreath, A paint-splattered easel, A vibrant sunflower with green leaves, Hot popcorn jump out from the red striped popcorn maker.

Table 1: Results of Text-to-3D on T³Bench dataset. Our proposed methods achieve state-of-the-art performance among 2D lifting methods, beating the diffusion based SDS and VSD priors.

Method	-	Dreamfusion (SDS) [14]	ProlificDreamer (VSD) [15]	RFDS	RFDS-Rev
Base Model	-	Diffusion	Diffusion	Rectified Flow	Rectified Flow
Single Object	Quality↑	24.9	51.1	46.9	57.6
	Alignment↑	24.0	47.8	46.8	52.5
	Average↑	24.4	49.4	46.9	55.1
Surroundings	Quality↑	19.3	42.5	34.5	44.6
	Alignment↑	29.8	47.0	51.0	62.0
	Average↑	24.6	44.8	42.8	53.3
Multiple Objects	Quality↑	17.3	45.7	28.3	44.6
	Alignment↑	14.8	25.8	24.5	34.3
	Average↑	16.1	35.8	26.4	39.5
Average	Average↑	21.7	43.3	38.7	49.3

based methods. Furthermore, the RFDS-Rev method sets a new state-of-the-art performance among all 2D lifting methods in this benchmark.

4.2 iRFDS vs. Rectified Flow Time Inversion vs. Diffusion Methods

We also study the performance of iRFDS in 2D image inversion and subsequent text-guided editing. Notably, a standard text-to-image rectified flow inherently supports the image-to-noise conversion due to its time-symmetric property. This can be achieved by simply reversing the flow from $t \rightarrow 1 - t$ and taking a negative velocity, a method we refer to as ‘Rectified Flow Time Inversion’. Unlike ‘Rectified Flow Time Inversion’, which is essentially the inverse of the generation process, our proposed iRFDS treats the noise as an optimization objective and uses the pretrained model as a loss function to optimize the noise using optimizers like SGD.

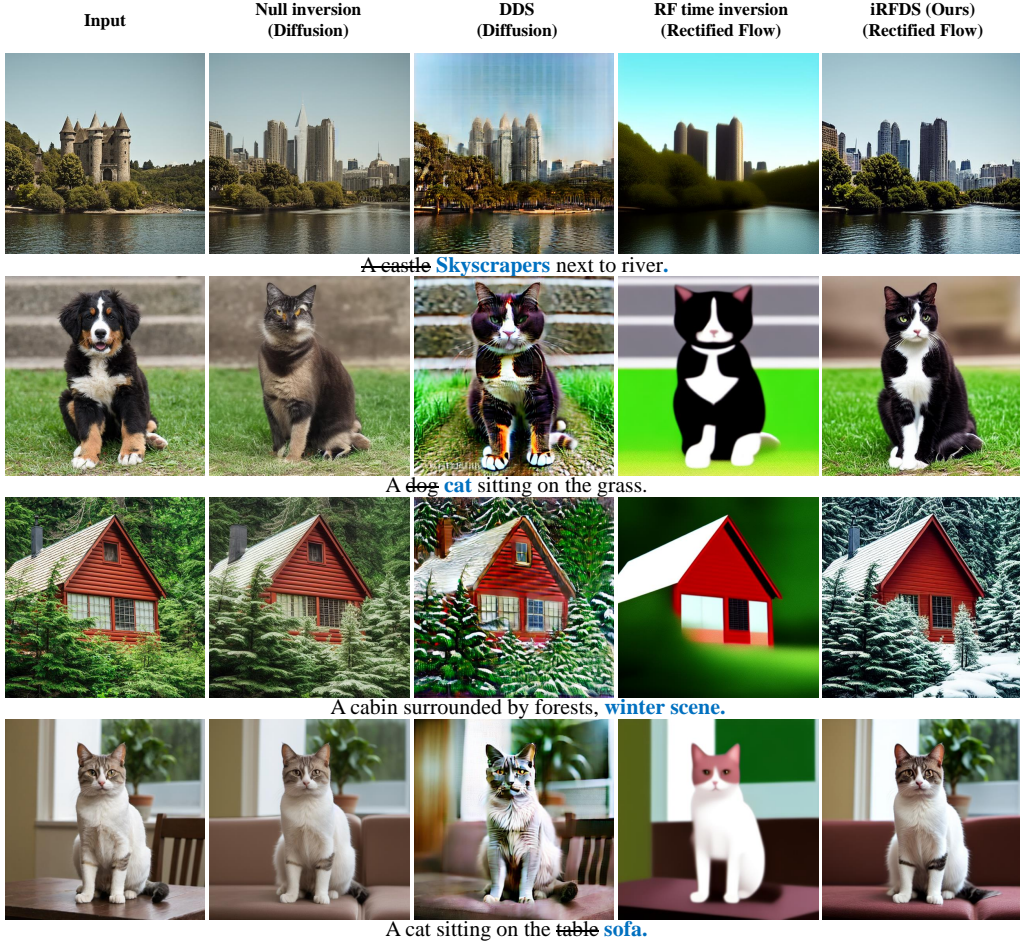


Figure 5: Comparison of 2D editing. Our iRFDS method is able to perform prompt-faithful editing.

Image inversion is also a widely explored topic in diffusion-based methods, known for its capability to edit real-world images. We compare iRFDS against the popular method – the null inversion method on real-world images. Additionally, we evaluate our method against the diffusion prior based optimization method, the DDS loss [17], which directly optimizes the original images.

The results of the inversion and editing are summarized in Fig. 5. We observe that “Rectified Flow Time Inversion” struggles to perform accurate inversions on real images. Compared to the diffusion-based null inversion, our proposed iRFDS method achieves very competitive performance. Meanwhile, the diffusion prior DDS loss tends to produce images with over-saturated colors. More visualization results can be found in Appendix.

To further validate the performance improvements, we conducted quantitative experiments to calculate the CLIP score between the target caption and the image after editing. Additionally, we carry out a user study to evaluate the editing performance from the users’ perspective. The experiments are performed on 15 real images collected from the internet, with each image being edited three times using different captions. The results are summarized in Table. 2. We observe that our proposed method iRFDS achieves the best performance in terms of CLIP scores and user preference.

Table 2: Quantitative comparison of 2D editing.

Method	DDS [17]	Null Inversion [28]	RF Time Inversion [20]	iRFDS (Ours)
CLIP Score	0.294	0.298	0.268	0.306
User Preference	12.8%	31.7%	0.0%	55.5%

4.3 Ablation Experiments

iRFDS optimization steps in RFDS-Rev (Algorithm 1). As demonstrated in Fig. 6, we show results from both the 2D case and 3D case. We observe that performing the iRFDS for 1 step achieves the best efficiency and performance trade-off.

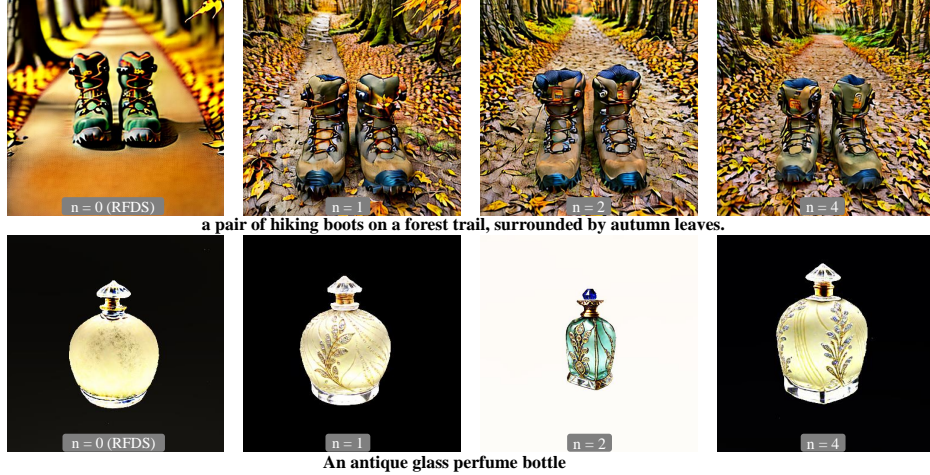


Figure 6: Experiments of the noise optimization step in RFDS-Rev. Top: 2D case. Bottom: 3D case. Optimizing the iRFDS for one step offers the optimal balance between efficiency and performance.

w/ Network Jacobian vs. w/o Network Jacobian. As illustrated in Fig. 7, we observe that keeping the network Jacobian can hardly generate meaningful images even at 2D case.



Figure 7: Ablation experiments of ignoring the Rf network Jacobian. We observe that it is difficult to generate images by keeping the Jacobian of the Rf network.

Additional Ablation Results. We also include additional ablation results in the Appendix. The experiments include: ablation on the effect of CFG, RFDS-Rev vs. directly applying the same idea of VSD to rectified flow and a comparison of computational cost between our methods and diffusion-based methods.

5 Discussion

Advantages over diffusion based methods. Besides the performance improvements, we observe that methods based on rectified flow achieve faster convergence during the optimization of 3D models. Intuitively, if we rearrange Eq. 6, x can be regarded as learning towards a direct objective $v_\phi + \epsilon$. In contrast, diffusion models rely on the difference in predicted noises to guide the optimization process, which is more circuitous. A detailed visual comparison is included in the Appendix.

6 Conclusion, Limitations and Broader Impacts

In this work, we introduce the SDS and VSD counterparts in rectified flow based methods. We propose three methods that utilize rectified flow as plug-and-play priors. Our two generative methods, RFDS and RFDS-Rev, outperform SDS and VSD in terms of text-to-3D generation. Additionally, the iRFDS method demonstrates robust capabilities in image inversion and text-guided editing.

Limitations. Since the 2D model lacks training with camera pose information, our proposed methods encounter similar issues to the SDS and VSD losses in 3D generation, such as the multi-face issue. These limitations can be addressed in future studies by training pose-aware models using multi-view data, similar to current diffusion based approaches [29; 30; 31; 32; 33].

Broader Impacts. Our approach significantly expands the potential applications of pretrained rectified flow models. We demonstrate that a text-to-image model can be adapted for both image editing and text-to-3D generation tasks. However, since we utilize pretrained text-to-image rectified flow models as our foundational network, our methods might also inherit the biases present in these base networks. For example, a model may predominantly depict professionals such as doctors or CEOs as males, thereby perpetuating existing societal stereotypes.

References

- [1] Jonathan Ho, Ajay Jain, and Pieter Abbeel. Denoising diffusion probabilistic models. *Advances in Neural Information Processing Systems*, 33:6840–6851, 2020.
- [2] Yang Song and Stefano Ermon. Generative modeling by estimating gradients of the data distribution. *Advances in neural information processing systems*, 32, 2019.
- [3] Yang Song and Stefano Ermon. Improved techniques for training score-based generative models. *Advances in neural information processing systems*, 33:12438–12448, 2020.
- [4] Robin Rombach, Andreas Blattmann, Dominik Lorenz, Patrick Esser, and Björn Ommer. High-resolution image synthesis with latent diffusion models. In *Proceedings of the IEEE/CVF Conference on Computer Vision and Pattern Recognition*, pages 10684–10695, 2022.
- [5] Prafulla Dhariwal and Alexander Nichol. Diffusion models beat gans on image synthesis. *Advances in neural information processing systems*, 34:8780–8794, 2021.
- [6] Jonathan Ho, Chitwan Saharia, William Chan, David J Fleet, Mohammad Norouzi, and Tim Salimans. Cascaded diffusion models for high fidelity image generation. *The Journal of Machine Learning Research*, 23(1):2249–2281, 2022.
- [7] Aditya Ramesh, Prafulla Dhariwal, Alex Nichol, Casey Chu, and Mark Chen. Hierarchical text-conditional image generation with clip latents. *arXiv preprint arXiv:2204.06125*, 2022.
- [8] Chitwan Saharia, William Chan, Saurabh Saxena, Lala Li, Jay Whang, Emily Denton, Seyed Kamyar Seyed Ghasemipour, Raphael Gontijo-Lopes, Burcu Karagol Ayan, Tim Salimans, et al. Photorealistic text-to-image diffusion models with deep language understanding. In *Advances in Neural Information Processing Systems*, 2022.
- [9] Yuwei Guo, Ceyuan Yang, Anyi Rao, Yaohui Wang, Yu Qiao, Dahua Lin, and Bo Dai. Animated-iff: Animate your personalized text-to-image diffusion models without specific tuning. *arXiv preprint arXiv:2307.04725*, 2023.
- [10] Andreas Blattmann, Tim Dockhorn, Sumith Kulal, Daniel Mendelevitch, Maciej Kilian, Dominik Lorenz, Yam Levi, Zion English, Vikram Voleti, Adam Letts, et al. Stable video diffusion: Scaling latent video diffusion models to large datasets. *arXiv preprint arXiv:2311.15127*, 2023.
- [11] Qingqing Huang, Daniel S Park, Tao Wang, Timo I Denk, Andy Ly, Nanxin Chen, Zhengdong Zhang, Zhishuai Zhang, Jiahui Yu, Christian Frank, et al. Noise2music: Text-conditioned music generation with diffusion models. *arXiv preprint arXiv:2302.03917*, 2023.
- [12] Ian Goodfellow, Jean Pouget-Abadie, Mehdi Mirza, Bing Xu, David Warde-Farley, Sherjil Ozair, Aaron Courville, and Yoshua Bengio. Generative adversarial nets. *Advances in neural information processing systems*, 27, 2014.
- [13] Alexandros Graikos, Nikolay Malkin, Nebojsa Jojic, and Dimitris Samaras. Diffusion models as plug-and-play priors. *Advances in Neural Information Processing Systems*, 35:14715–14728, 2022.

[14] Ben Poole, Ajay Jain, Jonathan T. Barron, and Ben Mildenhall. Dreamfusion: Text-to-3d using 2d diffusion. *arXiv*, 2022.

[15] Zhengyi Wang, Cheng Lu, Yikai Wang, Fan Bao, Chongxuan Li, Hang Su, and Jun Zhu. Prolific-dreamer: High-fidelity and diverse text-to-3d generation with variational score distillation. *arXiv preprint arXiv:2305.16213*, 2023.

[16] Xin Yu, Yuan-Chen Guo, Yangguang Li, Ding Liang, Song-Hai Zhang, and XIAOJUAN QI. Text-to-3d with classifier score distillation. In *The Twelfth International Conference on Learning Representations*, 2024. URL <https://openreview.net/forum?id=ktG8Tun1Cy>.

[17] Amir Hertz, Kfir Aberman, and Daniel Cohen-Or. Delta denoising score. *arXiv preprint arXiv:2304.07090*, 2023.

[18] Oren Katzir, Or Patashnik, Daniel Cohen-Or, and Dani Lischinski. Noise-free score distillation. In *The Twelfth International Conference on Learning Representations*, 2024. URL <https://openreview.net/forum?id=dLIMcm1Adk>.

[19] Xiaofeng Yang, Yiwen Chen, Cheng Chen, Chi Zhang, Yi Xu, Xulei Yang, Fayao Liu, and Guosheng Lin. Learn to optimize denoising scores for 3d generation. *arXiv:2312.04820*, 2023.

[20] Xingchao Liu, Chengyue Gong, and Qiang Liu. Flow straight and fast: Learning to generate and transfer data with rectified flow. *arXiv preprint arXiv:2209.03003*, 2022.

[21] Yaron Lipman, Ricky TQ Chen, Heli Ben-Hamu, Maximilian Nickel, and Matt Le. Flow matching for generative modeling. *arXiv preprint arXiv:2210.02747*, 2022.

[22] Michael S Albergo and Eric Vanden-Eijnden. Building normalizing flows with stochastic interpolants. *arXiv preprint arXiv:2209.15571*, 2022.

[23] Xingchao Liu, Xiwen Zhang, Jianzhu Ma, Jian Peng, and Qiang Liu. Instaflow: One step is enough for high-quality diffusion-based text-to-image generation. In *International Conference on Learning Representations*, 2024.

[24] Patrick Esser, Sumith Kulal, Andreas Blattmann, Rahim Entezari, Jonas Müller, Harry Saini, Yam Levi, Dominik Lorenz, Axel Sauer, Frederic Boesel, et al. Scaling rectified flow transformers for high-resolution image synthesis. *arXiv preprint arXiv:2403.03206*, 2024.

[25] Jonathan Ho and Tim Salimans. Classifier-free diffusion guidance. In *NeurIPS 2021 Workshop on Deep Generative Models and Downstream Applications*, 2022.

[26] Yuan-Chen Guo, Ying-Tian Liu, Ruizhi Shao, Christian LaForte, Vikram Voleti, Guan Luo, Chia-Hao Chen, Zi-Xin Zou, Chen Wang, Yan-Pei Cao, and Song-Hai Zhang. threestudio: A unified framework for 3d content generation. <https://github.com/threestudio-project/threestudio>, 2023.

[27] Yuze He, Yushi Bai, Matthieu Lin, Wang Zhao, Yubin Hu, Jenny Sheng, Ran Yi, Juanzi Li, and Yong-Jin Liu. T3bench: Benchmarking current progress in text-to-3d generation. *arXiv preprint arXiv:2310.02977*, 2023.

[28] Ron Mokady, Amir Hertz, Kfir Aberman, Yael Pritch, and Daniel Cohen-Or. Null-text inversion for editing real images using guided diffusion models. In *Proceedings of the IEEE/CVF Conference on Computer Vision and Pattern Recognition*, pages 6038–6047, 2023.

[29] Jianglong Ye, Peng Wang, Kejie Li, Yichun Shi, and Heng Wang. Consistent-1-to-3: Consistent image to 3d view synthesis via geometry-aware diffusion models. *arXiv preprint arXiv:2310.03020*, 2023.

[30] Ruoxi Shi, Hansheng Chen, Zhuoyang Zhang, Minghua Liu, Chao Xu, Xinyue Wei, Linghao Chen, Chong Zeng, and Hao Su. Zero123++: a single image to consistent multi-view diffusion base model. *arXiv preprint arXiv:2310.15110*, 2023.

[31] Weiyu Li, Rui Chen, Xuelin Chen, and Ping Tan. Sweetdreamer: Aligning geometric priors in 2d diffusion for consistent text-to-3d. *arXiv preprint arXiv:2310.02596*, 2023.

[32] Yichun Shi, Peng Wang, Jianglong Ye, Long Mai, Kejie Li, and Xiao Yang. Mvdream: Multi-view diffusion for 3d generation. *arXiv:2308.16512*, 2023.

[33] Xiaoxiao Long, Yuan-Chen Guo, Cheng Lin, Yuan Liu, Zhiyang Dou, Lingjie Liu, Yuexin Ma, Song-Hai Zhang, Marc Habermann, Christian Theobalt, et al. Wonder3d: Single image to 3d using cross-domain diffusion. *arXiv preprint arXiv:2310.15008*, 2023.

[34] Thomas Müller, Alex Evans, Christoph Schied, and Alexander Keller. Instant neural graphics primitives with a multiresolution hash encoding. *ACM Transactions on Graphics (ToG)*, 41(4):1–15, 2022.

A Appendix

A.1 Implementation Details

RFDS and RFDS-Rev for 3D generation. We use the large-scale rectified flow based text-to-image model InstaFlow [23] and the 3D model implicit model Instant-NGP [34]. Each 3D model is optimized for 15000 steps. We use a CFG of 50 for all 3D experiments and 2D toy experiments. The model is optimized with a resolution of 256 for the first 5000 steps and then 500 for the final 10000 steps. The experiments are carried out on NVIDIA A6000 GPUs. Generating one 3D scene using RFDS-Rev takes around 30 mins wall-clock time. We use $w(t) = 1$ in all experiments.

iRFDS for image inversion and editing. The inversion starts from a randomly sampled Gaussian noise. We optimize the noise for 1000 steps using iRFDS and CFG 1 with a learning rate of 3×10^{-3} . To facilitate effective noise optimization, we add one additional loss to enforce the noise follows a Gaussian distribution. Specifically, we add a loss to enforce the mean and variance of the current noise to be zero and one respectively. After the noise is optimized, we change the caption to the target caption and run the forward flow for 5 steps using CFG 1.5. We use $w(t) = 1$ in all experiments.

A.2 Additional Related Works

Diffusion as plug-and-play priors. Our work is greatly motivated by the development of diffusion based priors. The earliest work of diffusion prior [13] requires to backpropagate through the diffusion U-Net. Dreamfusion [14] recognizes that such a backpropagate process greatly hurt the performance of diffusion priors. By ignoring the U-Net Jacobian, the SDS loss proposed in Dreamfusion can be used for 3D generation and image editing. However, the initial version of the SDS loss suffers greatly from the lack of details and diversity. DDS loss [17] proposes an improved version of the SDS to improve image editing by taking the difference between the current SDS and the source image SDS. VSD loss improves the SDS loss for 3D generation problems. Specifically, it first trains a LoRA of the current 3D model and then takes the difference between the diffusion SDS and LoRA SDS. Although lots of methods have been proposed for diffusion models, this is the first work that studies how to effectively use rectified flow as priors.

A.3 Algorithm for RFDS and iRFDS

Algorithm 2: The RFDS Algorithm.

- 1 Initialize the learnable parameter θ
- 2 **while** Not Converge **do**
- 3 | Sample random timestep t
- 4 | Sample random noise ϵ
- 5 | Optimize θ with ϵ based on RFDS (Eq. 6)
- 6 **RETURN** θ

Algorithm 3: The iRFDS Algorithm.

- 1 Initialize the learnable parameter ϵ
- 2 Get initial image x
- 3 **while** Not Converge **do**
- 4 | Sample random timestep t
- 5 | Optimize ϵ using fixed x based on iRFDS (Eq. 8)
- 6 **RETURN** ϵ

A.4 Additional Ablation Experiments

Ablation Results on CFG. The scale of classifier-free guidance (CFG) [25] plays a crucial role in diffusion-based methods, such as SDS and VSD. We observe a very similar phenomenon with the

rectified flow priors. As demonstrated in Fig. 8, both of the proposed methods require a CFG greater than 10 to learn reasonable shapes. However, when the CFG becomes excessively large, the 3D objects generated by RFDS exhibit over-saturated colors. In contrast, RFDS-Rev remains robust to large CFG values, even when the CFG exceeds 2000.

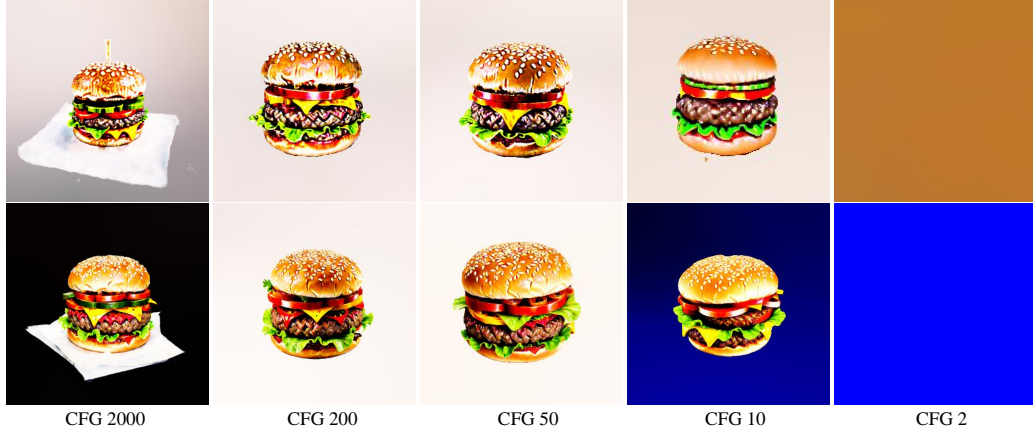


Figure 8: Ablation experiments of classifier free guidance scale on text-to-3D generation. Prompt: A DSLR image of a hamburger. Top: RFDS with different CFG. Bottom: RFDS-Rev.

RFDS-Rev vs. RFDS-VSD. As mentioned in the main text, some of the existing methods aimed at improving the diffusion models can be used directly on rectified flow based methods. We explore to combine VSD with the baseline RFDS, denoted as RFDS-VSD. Specifically, we train a rectified flow LoRA model based on the current rendered images and then calculate the gradients by taking the difference between RFDS and RFDS-LoRA following the VSD setting. Results are shown in Fig. 9. We observe that the RFDS-Rev generates much better results compared with RFDS-VSD, even though the VSD version requires more computations.



Figure 9: Ablation experiments of RFDS-Rev vs. RFDS-VSD. Top: 2D case. Bottom: 3D case.

A.5 Comparison of Convergence Speed with Diffusion-based Methods.

As listed in Fig. 10, we observe that our rectified flow based methods lead to much faster convergence speed when doing text-to-3D generation.

A.6 Comparison of the Computational Cost.

We evaluate the computational costs by examining the number of forward and backward passes of the diffusion or rectified flow network required in 1 optimization iteration. Results are list in Table. 3. The RFDS baseline has the same computational demands as the SDS loss. Due to the calculation of

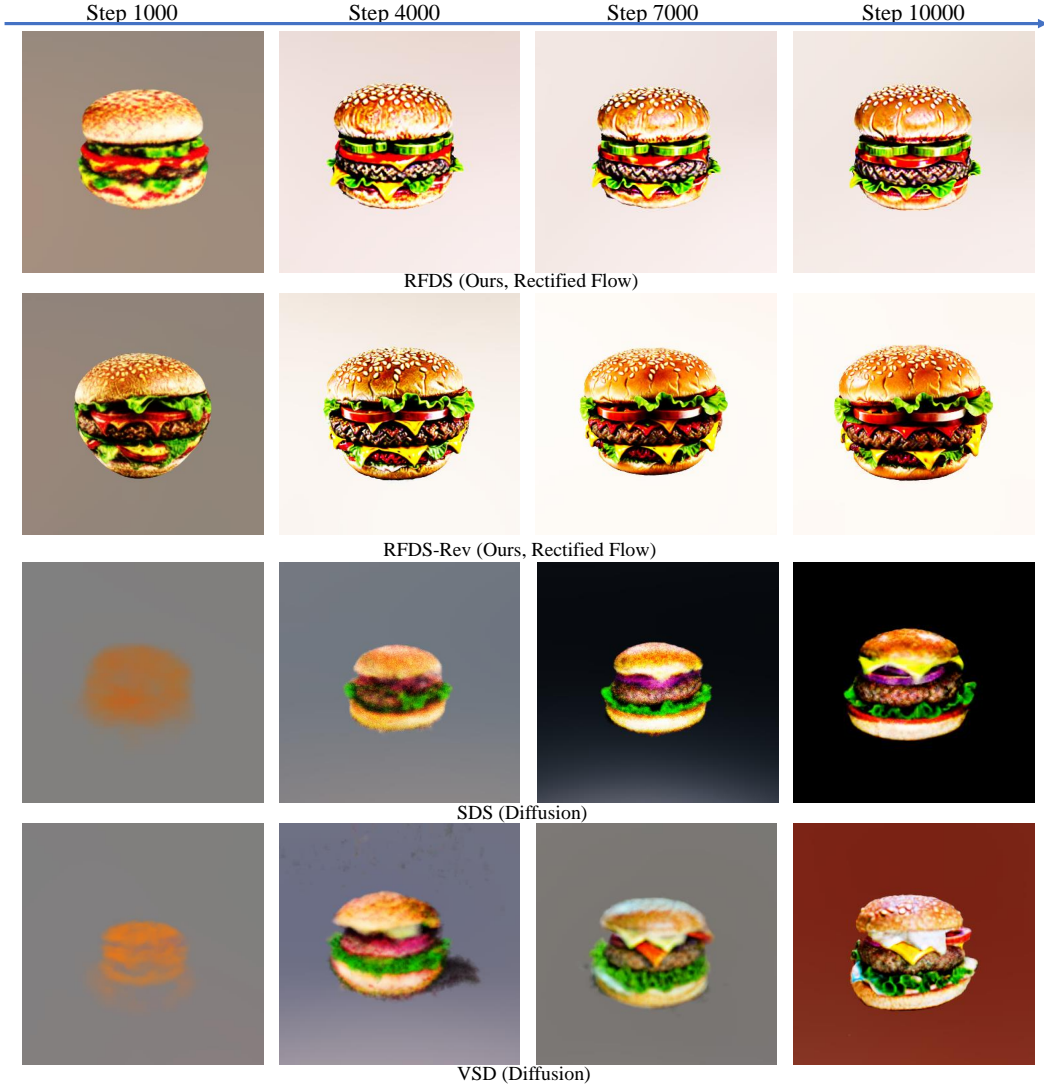


Figure 10: Comparison of convergence speed in 3D generation. Caption: A DSLR image of a hamburger. The 3D model is trained with the same learning rate. We observe that the rectified flow based methods converge much faster compared with diffusion-based methods.

CFG [25], they both require two forward passes. RFDS-Rev requires only one additional forward pass, whereas VSD needs two additional forward passes and one additional costly backward pass.

Table 3: Computational cost of one iteration based on the number of forward and backward passes of the network.

Method	SDS [14]	VSD [15]	DDS [17]	RFDS	iRFDS	RFDS-Rev
Category	-	Diffusion	Diffusion	Diffusion	Rectified Flow	Rectified Flow
Computation	Forward	2	4	2	2	3
	Backward	0	1	0	0	0

A.7 More results of image inversion and editing using iRFDS.

We show more results of 2D editing in Fig. 11.

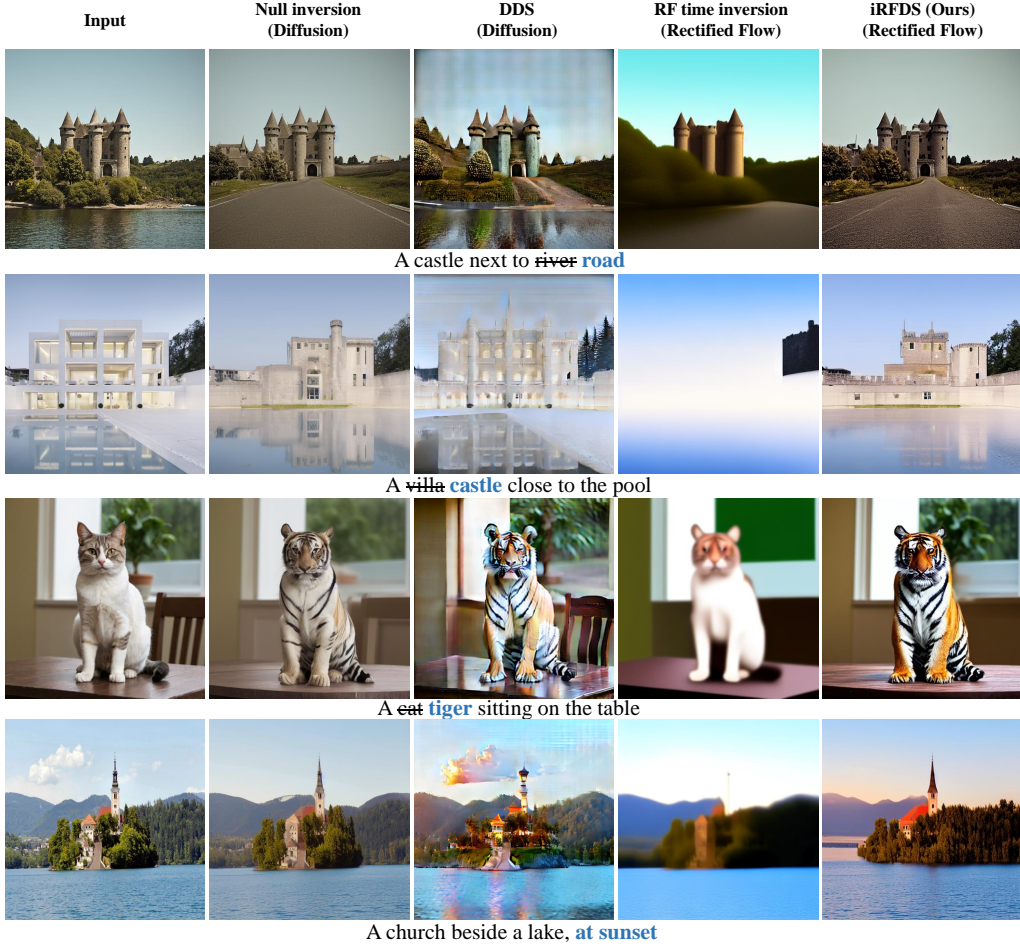


Figure 11: More results on 2D editing.

A.8 More results of text-to-3D generation

We show more qualitative results of text-to-3D generation in Fig. 12 and Fig. 13.

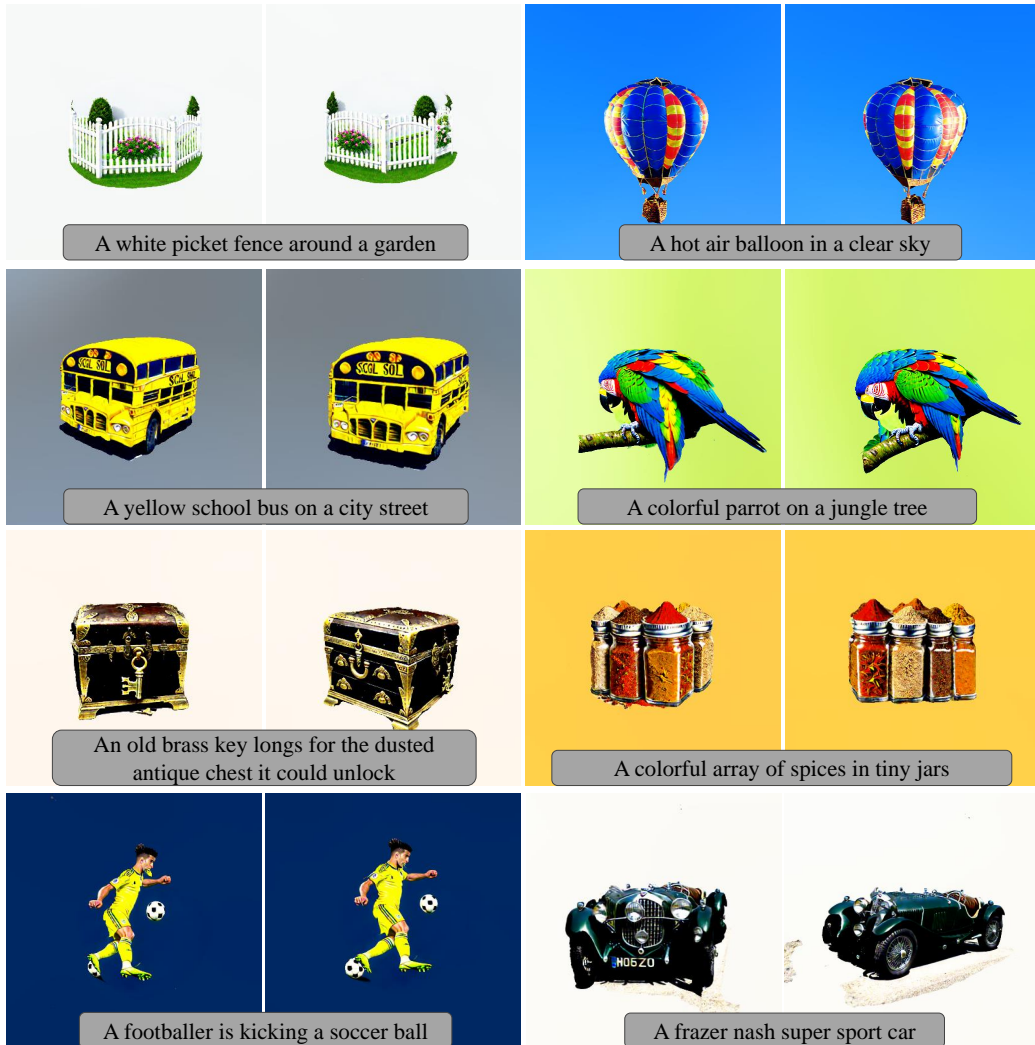
A.9 iRFDS user study details

The user study is carried out with google doc. The users are ask to select the best editing results from the 4 methods. A screenshot of the user study is shown in Fig 14.



Text-to-3D Generation with RFDS-Rev

Figure 12: More results on text-to-3D generation



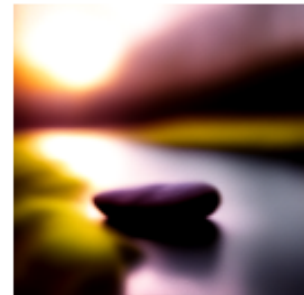
Text-to-3D Generation with RFDS-Rev

Figure 13: More results on text-to-3D generation

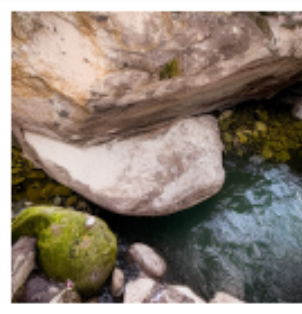
Given the source image: " a boat in a river ", which method is better by changing boat -> rock



Option 1



Option 2



Option 3



Option 4

Figure 14: User study screenshot